

# The Cation-Deficient Ruddlesden–Popper Oxysulfide $Y_2Ti_2O_5S_2$ as a Layered Sulfide: Topotactic Potassium Intercalation To Form $KY_2Ti_2O_5S_2$

Oliver J. Rutt, Timothy L. Hill, Zoltán A. Gál, Michael A. Hayward, and Simon J. Clarke\*

*Inorganic Chemistry Laboratory, Department of Chemistry, University of Oxford, South Parks Road, Oxford OX1 3QR, U.K.*

Received May 27, 2003

Potassium intercalation into the cation-deficient  $n = 2$  Ruddlesden–Popper oxysulfide  $Y_2Ti_2O_5S_2$  to form  $KY_2Ti_2O_5S_2$  has been carried out by reaction of the oxysulfide with potassium vapor in sealed metal tubes at 400 °C, potassium naphthalide in THF at 50 °C, or potassium in liquid ammonia at temperatures as low as  $-78$  °C. Insertion of potassium is topotactic, and although a site 12-coordinate by oxide ions is vacant in the perovskite-type oxide slabs of the structure, potassium is too large to enter this site via the 4-coordinate window, and instead enters the rock-salt-type sulfide layers of the structure which necessitates a 30% increase in the lattice parameter  $c$  normal to the layers. In contrast with one of the sodium intercalates of  $Y_2Ti_2O_5S_2$  ( $\beta$ - $NaY_2Ti_2O_5S_2$ ) in which sodium occupies a tetrahedral site in the sulfide layers, potassium favors an 8-coordinate site which necessitates a relative translation of adjacent oxide slabs.  $KY_2Ti_2O_5S_2$  is tetragonal:  $P4/mmm$ ,  $a = 3.71563(4)$  Å,  $c = 14.8682(2)$  Å (at 298 K),  $Z = 1$ . Although the resistivity ( $3.4(1) \times 10^3 \Omega$  cm) is larger than would be expected for a metal, temperature independent paramagnetism dominates the magnetic susceptibility, and the material is electronically very similar to the analogous sodium intercalate  $\beta$ - $NaY_2Ti_2O_5S_2$  which features reduced-titanium-containing oxide layers of very similar geometry and electron count.

## Introduction

Intercalation reactions carried out under mild conditions (“chimie douce” reactions) are important in the modification of solid state and materials properties.<sup>1–3</sup> Reductive topotactic insertion of alkali metals into transition metal oxides such as  $WO_3$ <sup>4</sup> and sulfides such as  $TiS_2$ <sup>5</sup> has been widely explored and is central to Li-ion battery technology.<sup>6</sup> Layered sulfides, oxyhalides,<sup>5,7</sup> and some layered oxides such as Ruddlesden–Popper (R–P) phases<sup>8</sup> (which consist of perovskite-type slabs separated by rock-salt-type layers) accept non-redox inter-

calants to increase the separation of the slabs<sup>9</sup> or exfoliate them.<sup>10</sup> Some R–P phases, such as  $Sr_3Ru_2O_7$ ,<sup>11</sup> undergo topotactic oxidative intercalation of fluorine into the rock-salt layers. We have recently demonstrated<sup>12</sup> that the layered oxysulfides with general formula  $Ln_2Ti_2O_5S_2$  ( $Ln = Pr$ – $Er$ ,  $Y$ ) reported independently by the groups of Tremel<sup>13</sup> and Meerschaut<sup>14</sup> may be reduced with concomitant insertion of an alkali metal cation. In these compounds, the oxide and sulfide anions order crystallographically, and the compounds formally consist of alternating  $[Ti_2O_5]^{2-}$  perovskite-like slabs, which contain a 12-coordinate vacant cation site, separated by  $[Ln_2S_2]^{2+}$  rock-salt-type layers. The reactivity of the compound  $Y_2Ti_2O_5S_2$ , which is the only member containing a diamagnetic trivalent cation, with alkali metal intercalants

\* To whom correspondence should be addressed. E-mail: simon.clarke@chem.ox.ac.uk. Fax: +44 1865 272690. Phone: +44 1865 272600.

(1) Murphy, D. W. *Adv. Synth. React. Solids* **1991**, *1*, 237.  
 (2) Rouxel, J.; Tournoux, M. *Solid State Ionics* **1996**, *84*, 141.  
 (3) Jacobson, A. J. In *Solid State Chemistry: Compounds*; Cheetham, A. K.; Day, P., Eds.; Clarendon Press, Oxford, 1992.  
 (4) Chippindale, A. M.; Dickens, P. G.; Powell, A. V. *Prog. Solid State Chem.* **1994**, *21*, 133.  
 (5) Eichhorn, B. W. In *Progress in Inorganic Chemistry*; Karlin, K. D., Ed.; Wiley: New York, 1994; Vol. 42.  
 (6) Bruce, P. G. *Chem. Commun.* **1997**, 1817.  
 (7) Palvadeau, P.; Coic, L.; Rouxel, J.; Portier, J. *Mater. Res. Bull.* **1978**, *13*, 221. Song, K.; Kauzlarich, S. M. *Chem. Mater.* **1994**, *6*, 386.  
 (8) Ruddlesden, S. N.; Popper, P. *Acta Crystallogr.* **1958**, *11*, 54.

(9) Mohan Ram, R. A.; Clearfield, A. J. *Solid State Chem.* **1994**, *112*, 288.  
 (10) Schaak, R. E.; Mallouk, T. E. *Chem. Mater.* **2000**, *12*, 3429.  
 (11) Li, R. K.; Greaves, C. *Phys. Rev. B* **2000**, *62*, 3811.  
 (12) Denis, S. G.; Clarke, S. J. *Chem. Commun.* **2001**, 2356.  
 (13) Goga, M.; Seshadri, R.; Ksenofontov, V.; Gütlich, P.; Tremel, W. *Chem. Commun.* **1999**, 979.  
 (14) Boyer, C.; Deudon, C.; Meerschaut, A. *C. R. Acad. Sci., Ser. II* **1999**, *2*, 93.

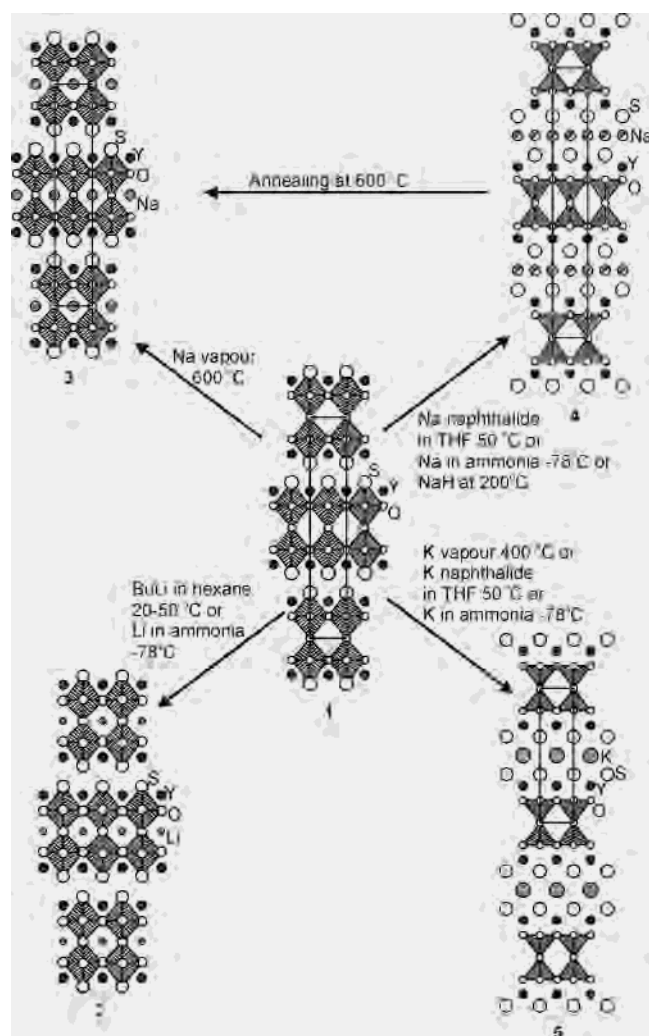


**Figure 1.** Scheme showing the structures of the materials derived from  $Y_2Ti_2O_5S_2$  (1) by intercalation of electropositive metals: The lithium intercalates  $Li_xY_2Ti_2O_5S_2$  ( $0 < x \leq 2$ )<sup>12,16</sup> (2), and the sodium intercalates  $\alpha-Na_xY_2Ti_2O_5S_2$  ( $0 < x \leq 1.0$ )<sup>12,15</sup> (3), obtained at temperatures of around 500–600 °C and containing the alkali metal ions in the oxide layers. In contrast, the room temperature sodium intercalate  $\beta-NaY_2Ti_2O_5S_2$  (4)<sup>12</sup> and the potassium intercalate  $KY_2Ti_2O_5S_2$  (5) described in this paper contain the alkali metal cations in the sulfide layers. Note that the half-shaded circles in 4 represent statistical occupancy of half of the available tetrahedral sites by sodium in this compound.

is summarized in the scheme in Figure 1, which includes the work presented here. Sodium may be inserted into either the 12-coordinate site in the perovskite-like oxide slab (under thermodynamic control) producing  $\alpha-Na_xY_2Ti_2O_5S_2$  ( $0 < x \leq 1$ )<sup>15</sup> or into a tetrahedral site in the sulfide layer (under kinetic control), producing  $\beta-NaY_2Ti_2O_5S_2$  (with no apparent range of compositions).<sup>12</sup> The intercalation of a reductant into the so-called rock-salt-type layers of a Ruddlesden–Popper phase was unprecedented, and the host material  $Y_2Ti_2O_5S_2$  behaves like an open framework oxide (e.g., like  $WO_3$ ) or like a layered sulfide (e.g.,  $TiS_2$ ) depending on the size of the alkali metal intercalants or on the reaction conditions. The alkali cations should always favor coordination by oxide, but whether this is achievable in topotactic insertion reactions, which are usually carried out at fairly

low temperatures (below about 500 °C), depends on the size and mobility of the cations. Thus, lithium always enters the oxide layers<sup>12</sup> and is of the appropriate size to occupy the 4-coordinate site<sup>16</sup> which is the “window” to the 12-coordinate vacancy in the oxide slabs in  $Y_2Ti_2O_5S_2$ . At temperatures of a few hundred degrees Celsius, sodium is sufficiently mobile to enter the oxide layers where it occupies the 12-coordinate site to produce  $\alpha-NaY_2Ti_2O_5S_2$  which has the ideal  $n = 2$  Ruddlesden–Popper stoichiometry. However, when sodium intercalation is carried out by means of reaction with sodium naphthalide in THF at 50 °C,<sup>12</sup> sodium in liquid ammonia at temperatures as low as –78 °C, or solid state reaction with sodium hydride at 200 °C, the metastable product  $\beta-NaY_2Ti_2O_5S_2$  is obtained with sodium statistically occupying half of the tetrahedral sites in the sulfide layers. In this paper, we describe the insertion of potassium (either using the vapor, potassium naphthalide or potassium/ammonia solution) and show that the even larger  $K^+$  ion insists on entering the sulfide layers and furthermore achieves 8-coordination by sulfur by means of translation of adjacent oxide slabs relative to one another in the  $ab$  plane. The structure of the oxide layers in  $KY_2Ti_2O_5S_2$  very closely resembles that of the analogous portion of the structure of  $\beta-NaY_2Ti_2O_5S_2$ , and since the electron counts are similar, the magnetic susceptibilities of the two materials are also similar. The syntheses of  $KY_2Ti_2O_5S_2$  and  $\beta-NaY_2Ti_2O_5S_2$  illustrate the potential for R–P sulfides or oxysulfides to behave like layered sulfides with reductive insertion into their rock-salt layers.

## Experimental Section

**Synthesis.**  $KY_2Ti_2O_5S_2$ , like  $\beta-NaY_2Ti_2O_5S_2$ ,<sup>12</sup> is extremely air-sensitive and oxidizes in a matter of seconds when exposed to air. All manipulations of solids were therefore carried out in a Glovebox Technology argon-filled recirculating drybox with a combined  $O_2$  and  $H_2O$  content of less than 5 ppm. Orange  $Y_2Ti_2O_5S_2$  was prepared on the 2–10 g scale by reacting stoichiometric quantities of  $Y_2O_3$ ,  $TiO_2$ , and  $TiS_2$  at 1100 °C in sealed silica tubes.  $Y_2O_3$  (Aldrich 99.99%) was dried at 900 °C for 24 h in air and then removed to the drybox, and  $TiO_2$  (Aldrich 99.9+ %) was dried at 250 °C in air;  $TiS_2$  was prepared by reacting Ti (ALFA 99.99%, dehydrided) with S (ALFA 99.9995%) at 600 °C for 3–4 days in evacuated silica tubes (caution: the temperature was raised slowly from 400 to 600 °C over 24 h to avoid a build-up of sulfur pressure). The starting materials were ground and loaded into a silica tube which had been baked at 900 °C under a vacuum of  $2 \times 10^{-2}$  mbar for several hours in order to remove adsorbed moisture. This prebaking step is important to minimize contamination of the oxysulfide with  $Y_2Ti_2O_7$ . The tube was sealed under a vacuum of  $2 \times 10^{-2}$  mbar, and the oxysulfide was obtained phase pure according to laboratory powder X-ray diffraction by heating at 1100 °C for 3–4 days. Following the example of sodium intercalation,<sup>12</sup> potassium intercalation was carried out using potassium vapor or using reducing solutions containing  $K^+$ . First,  $Y_2Ti_2O_5S_2$  powder was reacted with potassium vapor: a 4-fold molar excess (i.e.,  $K/Ti = 2:1$ ) of potassium (caution: excess potassium metal must be disposed of with great care after removal from the drybox, for

(15) Clarke, S. J.; Denis, S. G.; Rutt, O. J.; Hill, T. L.; Hayward, M. A.; Gál, Z. A. *Chem. Mater.*, submitted.

(16) Hyett, G.; Rutt, O. J.; Gál, Z. A.; Denis, S. G.; Hayward, M. A.; Clarke, S. J. *J. Am. Chem. Soc.*, submitted.

example by containing it in a Schlenk tube and adding propan-2-ol while maintaining a flow of  $N_2$  over the metal) was placed in a stainless steel tube (5 mm inner diameter, 3 cm long, welded closed at one end), and 2 g of  $Y_2Ti_2O_5S_2$  was placed in a nickel tube (Ni 222 alloy, 99.9% pure, 10 cm long, 9 mm inner diameter, 0.5 mm wall thickness and welded closed at one end). The stainless steel tube was then inserted inside the nickel tube such that the closed end of the steel tube was embedded in the  $Y_2Ti_2O_5S_2$  but that there would be no contact between molten potassium and the powder, providing the assembly was kept upright. The nickel tube was sealed by arc-welding under purified argon, and the whole was sealed in a silica jacket. The tube was placed upright in a chamber furnace and heated at 400 °C for 3–4 days. After cooling, the nickel tube was cut open in the drybox and the steel tube removed, and the powder, which was black at the top and still orange at the bottom of the nickel tube, was ground and replaced in the nickel tube along with the steel insert which still contained unreacted potassium. The procedure was repeated until the powder was homogeneous and dark blue-black in color and contained no unreacted  $Y_2Ti_2O_5S_2$  according to powder X-ray diffraction measurements. The second method of synthesis was analogous to that used to insert sodium into the rock-salt layers to produce  $\beta$ - $NaY_2Ti_2O_5S_2$ :<sup>12</sup> potassium naphthalide (0.05 M), prepared by reacting naphthalene dissolved in THF (which had been dried by distillation over potassium metal) with potassium metal under  $N_2$  with overnight stirring, was added to 2 g of  $Y_2Ti_2O_5S_2$ . The mixture was stirred at 50 °C for 1 week, and the excess naphthalide was then removed by filtration. The blue-black solid was washed three times with dry THF and dried under vacuum overnight prior to removal to the drybox. The naphthalide intercalation route was found in the case of  $\beta$ - $NaY_2Ti_2O_5S_2$  to result in the formation of a small amount of an impurity phase containing hydrogen and sodium as described in ref 12, most likely sodium hydride, NaH. Consequently, further low temperature routes to both  $\beta$ - $NaY_2Ti_2O_5S_2$  and  $KY_2Ti_2O_5S_2$  using the more strongly reducing alkali metal/ammonia solutions were also explored. A 2-fold molar excess of either sodium or potassium was dissolved in 30–50 cm<sup>3</sup> of alkali-metal-dried ammonia in one arm of a glass “H”-cell<sup>17</sup> (designed to withstand an internal pressure of up to 15 atm) and poured onto 0.5–3 g of  $Y_2Ti_2O_5S_2$  located in the other arm. The solution was stirred overnight at temperatures between –78 and +6 °C after which the powder had changed in color from orange to dark blue-black. The unreacted metal/ammonia solution was separated from the solid by means of a glass filter separating the two arms of the “H”-cell, and the solid was washed by condensing the ammonia back onto the solid and repeating the filtration step. The ammonia was then removed to another vessel, the “H”-cell evacuated to  $2 \times 10^{-2}$  mbar and the solid removed to the drybox. The thermal stability of  $KY_2Ti_2O_5S_2$  was investigated by heating 100 mg samples in predried, sealed silica ampules.

In the case of sodium intercalation, reduction using sodium hydride was performed: 0.2 g of  $Y_2Ti_2O_5S_2$  was ground together with a 2-fold molar excess of NaH (Aldrich, dry, 95%). The mixture was sealed in a Pyrex tube and heated at 200 °C for several periods of 24 h with intermediate regrinding. The solid phases present were  $\beta$ - $NaY_2Ti_2O_5S_2$ , along with unreacted  $Y_2Ti_2O_5S_2$  and NaH. It was found difficult to effect complete conversion to  $\beta$ - $NaY_2Ti_2O_5S_2$  using this route.

**Chemical Analysis.** Analysis for alkali metal content was carried using a Thermo Elemental Atomscan 16 ICP analyzer. Potassium or sodium ions were leached out of the intercalates by placing the

materials in deionized water; the solids rapidly turned yellow-brown, and the solutions were analyzed for  $K^+$  or  $Na^+$  after a few days of hydrolysis.

**Diffraction Measurements.** Powder X-ray diffraction (PXRD) measurements to assess phase purity and determine lattice parameters were carried out using a Siemens D5000 diffractometer operating in Debye–Scherrer geometry with  $Cu K\alpha_1$  radiation selected using a Ge(111) monochromator. The sample was ground with amorphous boron (1:1 mass ratio) to limit sample absorption and sealed in a 1 mm diameter glass capillary. Powder neutron diffraction (PND) measurements were carried out using the diffractometer POLARIS at the ISIS Facility, Rutherford Appleton Laboratory, U.K. A sample of approximately 2 g in mass obtained using the vapor intercalation route was measured at 298 and 2 K (achieved using an ILL “orange” cryostat) in the  $d$ -spacing range  $0.4 < d < 8 \text{ \AA}$  by means of three banks of detectors located at scattering angles  $2\theta$  of 35° ( $^3He$  tube detector), 90° (ZnS scintillator), and 145° ( $^3He$  tube detector, highest resolution bank:  $\Delta d/d = 5 \times 10^{-3}$ ) for total integrated proton currents at the production target of 534  $\mu Ah$  at 298 K and 684  $\mu Ah$  at 2 K. The sample was contained in a 10 mm diameter thin-walled vanadium can which was sealed in the drybox with an indium gasket. Simultaneous Rietveld refinement against data from all three detector banks was carried out using the GSAS suite of programs.<sup>18</sup>

**Magnetic Susceptibility Measurements.** Measurements were carried out using a Quantum Design MPMS2 SQUID magnetometer in the temperature range 5–320 K at magnetic fields of up to 5 T. A 50–80 mg portion of material was loaded into predried (100 °C) gelatin capsules which were sealed with superglue immediately after removal from the drybox and then immediately loaded into the magnetometer to avoid degradation of the samples due to the permeability of the gelatin capsules. Measurements of the susceptibility were made at each temperature by measuring the moment of the sample at fields of 4 and 5 T and determining the gradient of moment against field in this region. This was necessary because measurements of sample moment against field showed that the samples, which have small paramagnetic moments, usually contained minuscule amounts of ferromagnetic impurities (probably nickel) which saturated at fields above 1 T. Corrections were carried out for core diamagnetism using standard tables.<sup>19</sup>

## Results and Discussion

PXRD measurements showed that the products of sodium intercalation using sodium/ammonia solution or sodium hydride had lattice parameters identical to those of the material previously reported and prepared by the naphthalide route.<sup>12</sup> There was no effect of synthesis temperature on the products of reaction with sodium/ammonia solution.  $\beta$ - $NaY_2Ti_2O_5S_2$  prepared by this route at –78 °C analyzed as  $Na_{1.10(5)}Y_2Ti_2O_5S_2$ , consistent with the composition obtained from PND measurements on sodium naphthalide-derived material, which contained some NaH,<sup>12</sup> and indicating a Ti oxidation state of +3.5. In the case of potassium intercalation, the products of all three (potassium vapor, potassium naphthalide, and potassium/ammonia (at –78 or +6 °C)) reactions were fine blue-black powders. PXRD measurements indicated that materials made by all three routes had identical

(17) Wayda, A. L.; Dye, J. L. *J. Chem. Educ.* **1985**, *62*, 356.

(18) Larson, A.; von Dreele, R. B. *The General Structure Analysis System*; Los Alamos National Laboratory: Los Alamos, NM, 1985.

(19) *Magnetic Properties of Transition Metal Compounds, Supplement 2*; Landolt-Bornstein New Series II/10; Springer-Verlag: Berlin, 1979.

lattice parameters and that the insertion of potassium appeared to be topotactic, but that it involved a dramatic increase in the  $c$  lattice parameter perpendicular to the layers. Material prepared by vapor intercalation was used in subsequent structural investigations. Chemical analysis for potassium carried out on several samples prepared by the vapor intercalation route and the softer routes produced a mean composition of  $K_{0.96(3)}Y_2Ti_2O_5S_2$  ( $Ti^{3.5+}$ ). Investigation of the stability of this phase at temperatures greater than that used for the vapor intercalation showed that, after heating for 2 days at 600 °C, the material had begun to lose crystallinity. After treatment at 800 °C for 2 days, the only crystalline phase identifiable using PXRD was  $Y_2Ti_2O_7$ .

Close inspection of laboratory powder diffraction patterns indicated that the model obtained for the sodium intercalate  $\beta$ - $NaY_2Ti_2O_5S_2$ <sup>12</sup> in the body centered tetragonal space group  $I4/mmm$  was not appropriate to the potassium intercalate. The PXRD pattern of  $KY_2Ti_2O_5S_2$  was indexed on a primitive tetragonal cell with similar basal dimensions to those of  $Y_2Ti_2O_5S_2$  and  $\beta$ - $NaY_2Ti_2O_5S_2$ , but reflections identified as  $00l$  were almost coincident with those identified as  $00\frac{1}{2}$  in  $\beta$ - $NaY_2Ti_2O_5S_2$ . These observations are consistent with an expansion of the structure perpendicular to the layers of around 30% compared with  $Y_2Ti_2O_5S_2$ , similar to that observed for  $\beta$ - $NaY_2Ti_2O_5S_2$ <sup>12</sup> indicating insertion of  $K^+$  into the sulfide layers; the loss of body centering is consistent with the assumption that the  $K^+$  ion would adopt 8-coordination, rather than the tetrahedral 4-coordination of  $Na^+$  in  $\beta$ - $NaY_2Ti_2O_5S_2$ <sup>12</sup> and force a shift of adjacent oxide layers relative to one another by  $\frac{1}{2}$  in the  $x$  and  $y$  directions. This model was found to satisfactorily reproduce the intensity of the reflections in the X-ray diffraction patterns of  $KY_2Ti_2O_5S_2$  and was used as the starting model for refinement against PND data. Refinement of this model in space group  $P4/mmm$  against PND data collected on POLARIS confirmed that the relative shift in adjacent oxide layers had indeed occurred so that the potassium ion achieved square prismatic 8-coordination. The refinements at 298 and 2 K proceeded without incident apart from the need to include terms in the profile function which accounted for slight anisotropic peak broadening (the  $hkl$  reflections were slightly broader than the  $00l$  reflections). There was no evidence for preferred orientation despite the layered nature of the material. Two low-intensity peaks from an unidentified impurity phase were excluded from the refinement. The fit to the diffraction pattern collected at 298 K is shown in Figure 2, the refinement results are presented in Table 1, and the atomic coordinates obtained at 298 and 2 K are shown in Table 2. The large  $d$ -spacing range available on POLARIS allows refinement of anisotropic displacement ellipsoids, and this was carried out at 298 K for all atoms apart from Ti. Ellipsoids at 2 K were refined isotropically. According to the refinements, the potassium ion fully occupies the 8-coordinate site in the sulfide layer, and the refined composition of  $K_{0.99(1)}Y_2Ti_2O_5S_2$  is in excellent agreement with the composition obtained by chemical analysis.

The environment of titanium, which is formally in the +3.5 oxidation state, is similar to that found for  $\beta$ - $NaY_2Ti_2O_5S_2$ <sup>12</sup>

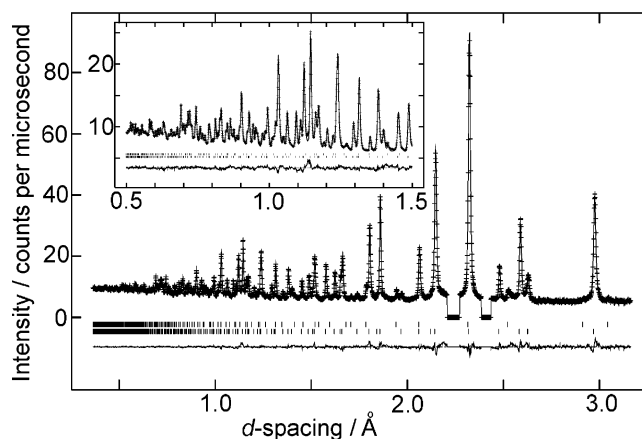


**Figure 2.** Rietveld refinements against powder neutron diffraction data ( $2\theta = 145^\circ$ ) for  $KY_2Ti_2O_5S_2$ , at room temperature,  $\chi^2 = 2.31$ ,  $wR_p = 0.0196$ ,  $R(F^2) = 0.0273$ ; tick marks are for  $KY_2Ti_2O_5S_2$  (bottom), and 1 mol % of  $Y_2Ti_2O_7$  impurity (top). Excluded regions contain low intensity broad reflections arising from small amounts of an unidentified impurity phase. The inset shows a magnification of the low  $d$ -spacing region.

**Table 1.** Refinement Results for  $KY_2Ti_2O_5S_2$  at Room Temperature and 2 K<sup>a</sup>

	$KY_2Ti_2O_5S_2$	$KY_2Ti_2O_5S_2$
formula	$KY_2Ti_2O_5S_2$	$KY_2Ti_2O_5S_2$
radiation	neutron	neutron
instrument	POLARIS	POLARIS
T/K	298	2
space group	$P4/mmm$	$P4/mmm$
fw	456.84	456.84
$a/\text{Å}$	3.71562(4)	3.70213(6)
$c/\text{Å}$	14.8682(2)	14.8104(3)
$V/\text{Å}^3$	205.268(7)	202.988(9)
Z	1	1
$\rho_{\text{calc}}/\text{Mg m}^{-3}$	4.971(1)	5.027(1)
no. variables	116	103
$\chi^2$	2.31	2.43
$wR_p^b$	0.0196	0.0109
$R_p^b$	0.0335	0.0174
$R(F^2)^b$	0.0273	0.0271

<sup>a</sup> All refinements were carried out against data from the three detector banks on POLARIS at  $145^\circ$ ,  $90^\circ$ , and  $35^\circ$   $2\theta$ . <sup>b</sup>  $R$  factors are given for all data.

**Table 2.** Atomic Parameters for  $KY_2Ti_2O_5S_2$  from Refinement in  $P4/mmm$  against Neutron Diffraction Data<sup>a</sup>

atom	site	$x$	$y$	$z$	$100 \times U_{\text{iso,eq}}/\text{Å}^2$	fractional occupancy
Y	2h	0.5 (0.5)	0.5 (0.5)	0.25826(3) (0.25937(4))	0.48(1) (0.14(1))	
Ti	2g	0 (0)	0 (0)	0.12244(8) (0.1229(1))	0.37(1) (0.09(2))	
O1	4i	0.5 (0.5)	0 (0)	0.16716(3) (0.16775(4))	0.46(2) (0.17(1))	
O2	1a	0 (0)	0 (0)	0 (0)	1.99(5) (1.20(3))	
S	2g	0 (0)	0 (0)	0.34904(9) (0.3510(1))	0.65(5) (0.14(3))	
K	1d	0.5 (0.5)	0.5 (0.5)	0.5 (0.5)	3.03(8) (0.75(3))	0.99(1) 1.0 <sup>b</sup>

<sup>a</sup> Room temperature and 2 K (in parentheses) results are given. Equivalent isotropic displacement parameters are given:  $U_{\text{iso,eq}}$  is one-third of the trace of the orthogonalized  $U_{ij}$  tensor, and anisotropic displacement parameters are shown as ellipsoids in Figure 3. <sup>b</sup> Not refined.

The bond distances and angles for the latter material are presented for comparison in Table 3. The intercalation of sodium and potassium into the sulfide layers is topotactic and reversible: exposure to moisture restores the original

**Table 3.** Selected Bond Distances (Å) and Angles (deg) for  $\text{KY}_2\text{Ti}_2\text{O}_5\text{S}_2$  at Room Temperature and 2 K<sup>a</sup>

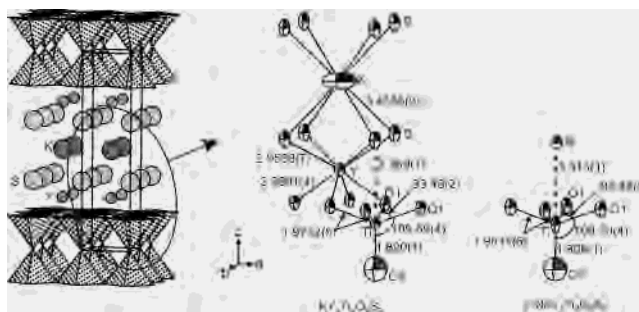
bond	$\text{KY}_2\text{Ti}_2\text{O}_5\text{S}_2$	$\text{KY}_2\text{Ti}_2\text{O}_5\text{S}_2$	$\beta\text{-NaY}_2\text{Ti}_2\text{O}_5\text{S}_2$	$\text{Y}_2\text{Ti}_2\text{O}_5\text{S}_2$
	298 K/Å	2 K/Å	298 K/Å	298 K/Å
Ti–O1 [4]	1.9732(5)	1.9666(6)	1.9814(6)	1.9427(1)
Ti–O2 [1]	1.820(1)	1.820(2)	1.809(1)	1.7941(4)
Y–O1 [4]	2.2991(4)	2.2952(6)	2.3008(5)	2.4277(2)
Y–S [4]	2.9538(7)	2.9486(9)	2.9404(7)	2.8048(2)
Y–S [1]				2.9395(6)
K–S [8]	3.4555(9)	3.424(1)		
Na–S [4]			2.796(1)	

angle	$\text{KY}_2\text{Ti}_2\text{O}_5\text{S}_2$	$\text{KY}_2\text{Ti}_2\text{O}_5\text{S}_2$	$\beta\text{-NaY}_2\text{Ti}_2\text{O}_5\text{S}_2$	$\text{Y}_2\text{Ti}_2\text{O}_5\text{S}_2$
	298 K/deg	2 K/deg	298 K/deg	298 K/deg
O1–Ti–O2 [4]	109.69(4)	109.74(5)	109.70(4)	104.03(1)
O1–Ti–O1 [2]	140.61(7)	140.52(9)	140.60(9)	151.95(3)
O1–Ti–O1 [4]	83.48(2)	83.45(3)	83.48(3)	86.633(6)

<sup>a</sup> Comparisons with analogous bond lengths and angles in  $\beta\text{-NaY}_2\text{Ti}_2\text{O}_5\text{S}_2$  and  $\text{Y}_2\text{Ti}_2\text{O}_5\text{S}_2$  (both from results described in ref 12) are also given. The numbers in square brackets indicate the number of bonds or angles of a particular type.

structure of  $\text{Y}_2\text{Ti}_2\text{O}_5\text{S}_2$ . However, insertion into this layer appears surprising: in  $\text{Y}_2\text{Ti}_2\text{O}_5\text{S}_2$ , the yttrium ion is 9-coordinate, and the interlamellar Y–S distance of 2.9395(6) Å is similar to the sum of the ionic radii ( $\text{Y}^{3+} = 1.08$  Å and  $\text{S}^{2-} = 1.84$  Å)<sup>20</sup> and only slightly longer than the other four Y–S bonds of 2.8048(2) Å. Yttrium is additionally coordinated by four oxide ions 2.4277(2) Å distant. However, in  $\beta\text{-NaY}_2\text{Ti}_2\text{O}_5\text{S}_2$  and  $\text{KY}_2\text{Ti}_2\text{O}_5\text{S}_2$ , the yttrium ion is 8-coordinate, and there is no interlamellar Y–S bonding. Accompanying this change in the coordination environment of the yttrium ion is a change in the coordination of the titanium ion. In  $\text{Y}_2\text{Ti}_2\text{O}_5\text{S}_2$ , Ti is coordinated by five oxide ions<sup>12</sup> (Table 3), and the sixth coordination site is occupied by sulfur, although this is located 2.8741(6) Å distant, approximately 0.4 Å longer than would be expected on the basis of the sum of the ionic radii and by comparison with  $\text{TiS}_2$  (Ti–S = 2.43 Å × 6),<sup>21</sup> but still indicative of some Ti–S bonding.<sup>13,14,22</sup> In  $\beta\text{-NaY}_2\text{Ti}_2\text{O}_5\text{S}_2$  and  $\text{KY}_2\text{Ti}_2\text{O}_5\text{S}_2$ , this Ti–S distance is much larger (3.313(1) and 3.369(1) Å, respectively) and can no longer be considered even a long bonding distance. In these intercalates, therefore, titanium is unambiguously coordinated only by five oxide ions (Table 3) in a square pyramidal geometry as shown in Figure 3. The angle between the basal and apical Ti–O bonds increases from 104.03(1)° in  $\text{Y}_2\text{Ti}_2\text{O}_5\text{S}_2$  to 109.70(4)° in  $\beta\text{-NaY}_2\text{Ti}_2\text{O}_5\text{S}_2$  and an almost identical 109.69(4)° in  $\text{KY}_2\text{Ti}_2\text{O}_5\text{S}_2$ . This change in the coordination environment of titanium is in contrast with the shortening of the Ti–S bond (to 2.732(3) Å) and the decrease in the angle between the basal and apical Ti–O bonds (to 99.25(6)°) observed when sodium intercalates into the oxide layers to form  $\alpha\text{-NaY}_2\text{Ti}_2\text{O}_5\text{S}_2$ ,<sup>12,15</sup> and with similar changes which accompany intercalation of lithium into the oxide layers.<sup>16</sup> These changes in coordination environment are consistent with the competition between the cations for the



**Figure 3.** Structure of  $\text{KY}_2\text{Ti}_2\text{O}_5\text{S}_2$  derived from refinement against powder neutron diffraction data. Double layers,  $\text{Ti}_2\text{O}_5$ , of all-corner-linked  $\text{TiO}_5$  square pyramids intergrow with  $\text{KS}_2$  layers in which K is in square prismatic coordination by S. The two types of layers are joined by  $\text{Y}^{3+}$  ions which are in square antiprismatic coordination ( $4 \times \text{S}$  and  $4 \times \text{O1}$ ). Bond distances are in ångströms, and angles are in degrees. The Ti environment in  $\beta\text{-NaY}_2\text{Ti}_2\text{O}_5\text{S}_2$ <sup>12</sup> is shown for comparison. Displacement ellipsoids are shown at the 99% level.

sulfide or oxide anions in the two cases. In all the intercalates, the lengths of the Ti–O bonds increase. In the case of  $\text{KY}_2\text{Ti}_2\text{O}_5\text{S}_2$  considered here, the basal Ti–O bonds increase by 1.57(4)% from 1.9427(1) Å in  $\text{Y}_2\text{Ti}_2\text{O}_5\text{S}_2$  to 1.9732(5) Å in  $\text{KY}_2\text{Ti}_2\text{O}_5\text{S}_2$ , and the apical Ti–O bond increases by 1.50(8)% from 1.7941(4) Å in  $\text{Y}_2\text{Ti}_2\text{O}_5\text{S}_2$  to 1.821(1) Å in  $\text{KY}_2\text{Ti}_2\text{O}_5\text{S}_2$ . This is a consequence of the insertion of electrons into bands which are Ti–O  $\pi$ -antibonding in nature. The Ti–O bond lengths in  $\text{KY}_2\text{Ti}_2\text{O}_5\text{S}_2$  are similar to those in  $\beta\text{-NaY}_2\text{Ti}_2\text{O}_5\text{S}_2$ <sup>12</sup> (Table 3), so despite the very different coordinations of the alkali metals in the sulfide layers, the similar electron counts of the two compounds dictate that the oxide slabs have very similar geometries. The molar magnetic susceptibilities are expected to be strongly dependent on the geometry of the oxide slabs: comparison of the susceptibilities for  $\text{KY}_2\text{Ti}_2\text{O}_5\text{S}_2$  and  $\beta\text{-NaY}_2\text{Ti}_2\text{O}_5\text{S}_2$  samples prepared using the different synthetic routes is shown in Figure 4. This shows that samples of  $\text{KY}_2\text{Ti}_2\text{O}_5\text{S}_2$  and  $\beta\text{-NaY}_2\text{Ti}_2\text{O}_5\text{S}_2$  have quantitatively similar magnetic susceptibilities when prepared by the same synthetic route. Samples prepared using the vapor intercalation route ( $\text{KY}_2\text{Ti}_2\text{O}_5\text{S}_2$  only) or intercalation using alkali metal ammonia solution over a period of 24 h at  $-78$  °C (both  $\text{KY}_2\text{Ti}_2\text{O}_5\text{S}_2$  and  $\beta\text{-NaY}_2\text{Ti}_2\text{O}_5\text{S}_2$ ) have susceptibilities of around  $1 \times 10^{-3}$  emu mol<sup>-1</sup> which are almost independent of temperature suggesting that these materials are Pauli paramagnets with delocalized electrons. In contrast, samples of  $\text{KY}_2\text{Ti}_2\text{O}_5\text{S}_2$  and  $\beta\text{-NaY}_2\text{Ti}_2\text{O}_5\text{S}_2$  prepared using alkali metal naphthalide solutions at 50 °C for 2 weeks have susceptibilities which are similar to each other, but which contain a small Curie term in addition to a dominant temperature independent term. The temperature independent terms are of similar order to those in the samples prepared by the vapor or alkali metal/ammonia routes, and fits of the susceptibilities<sup>12</sup> to  $\chi = \chi_0 + C/T$  (where  $\chi_0$  is the temperature independent term and  $C$  is the Curie constant) for the two naphthalide-derived materials show that around 5–10% of the Ti ions behave as  $S = 1/2$  moments in these cases. The observation that the samples prepared by the naphthalide route contain a significant concentration of impurity spins suggests that the vigorous and prolonged stirring of the

(20) Shannon, R. D. *Acta Crystallogr.* **1976**, A32, 751.

(21) Dahn, J. R.; McKinnon, W. R.; Haering, R. R.; Buyers, W. J. L.; Powell, B. M. *Can. J. Phys.* **1980**, 58, 207.

(22) Lafond, A.; Leynaud, O.; André, G.; Bourée, F.; Meerschaut, A. J. *Alloys Compd.* **2002**, 338, 185.

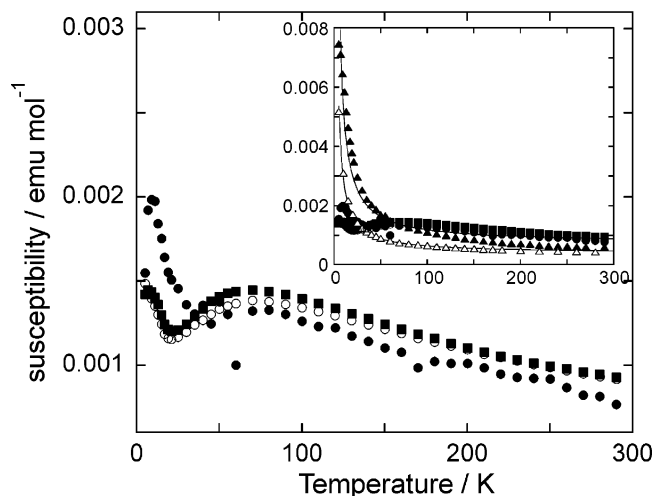


**Figure 4.** Magnetic susceptibilities for samples of  $\text{KY}_2\text{Ti}_2\text{O}_5\text{S}_2$  and  $\beta\text{-NaY}_2\text{Ti}_2\text{O}_5\text{S}_2$  prepared from  $\text{Y}_2\text{Ti}_2\text{O}_5\text{S}_2$  by different synthetic routes. The main figure shows almost temperature independent susceptibilities for samples of  $\text{KY}_2\text{Ti}_2\text{O}_5\text{S}_2$  prepared using potassium/ammonia solution (■) and potassium vapor (●), and a sample of  $\beta\text{-NaY}_2\text{Ti}_2\text{O}_5\text{S}_2$  prepared using sodium/ammonia solution (○). The inset shows additionally the susceptibilities of samples of  $\text{KY}_2\text{Ti}_2\text{O}_5\text{S}_2$  (▲) and  $\beta\text{-NaY}_2\text{Ti}_2\text{O}_5\text{S}_2$ <sup>12</sup> (△) prepared using the alkali metal naphthalides in THF. The fits in the inset are to  $\chi = \chi_0 + C/T$  with Curie constants corresponding to 5% (for  $\beta\text{-NaY}_2\text{Ti}_2\text{O}_5\text{S}_2$ ) and 9% (for  $\text{KY}_2\text{Ti}_2\text{O}_5\text{S}_2$ ) of Ti ions behaving as  $S = 1/2$  moments.

samples in suspension is responsible for generating the impurity spins, possibly in the form of surface states. The susceptibility results emphasize that the similarities in the crystal structures and electron counts of  $\text{KY}_2\text{Ti}_2\text{O}_5\text{S}_2$  and  $\beta\text{-NaY}_2\text{Ti}_2\text{O}_5\text{S}_2$  result in very similar band structures and electronic behavior, and that adjacent oxide slabs are electronically isolated from one another. Direct measurements of the electronic conductivities are hampered by the air sensitivity of the materials, and the decomposition (for  $\text{KY}_2\text{Ti}_2\text{O}_5\text{S}_2$ ) or structural change (for  $\beta\text{-NaY}_2\text{Ti}_2\text{O}_5\text{S}_2$ )<sup>12</sup> on heating the materials above 600 °C which prevents sintering of the powders. Measurement of the resistivity of a cold-

pressed pellet of the potassium-vapor-derived material used for the neutron diffraction investigation produced a value of  $3.4(1) \times 10^3 \Omega \text{ cm}$ , and values of  $4.4(5) \times 10^4$  and  $1.5(5) \times 10^5 \Omega \text{ cm}$  were obtained for alkali metal/ammonia-derived  $\text{KY}_2\text{Ti}_2\text{O}_5\text{S}_2$  and  $\beta\text{-NaY}_2\text{Ti}_2\text{O}_5\text{S}_2$ , respectively. These values are rather larger than one would expect for metallic materials, although the intergrain resistance in a nonsintered material will make a major contribution to the resistivity, particularly in an electronically anisotropic compound.

## Conclusion

The term “rock-salt layers” used to refer to the layers which separate the perovskite-related slabs in the Ruddlesden–Popper family of structures suggests that such layers are structurally robust. However, the ready exfoliation of some of these compounds,<sup>9</sup> and the topotactic oxidative insertion of fluorine<sup>11</sup> or reductive insertion of alkali metals,<sup>12</sup> described here, into these rock salt layers, emphasizes the two-dimensional nature of these compounds. In its reactions with sources of sodium and potassium,  $\text{Y}_2\text{Ti}_2\text{O}_5\text{S}_2$  resembles a layered sulfide. Attempts to reduce compounds with sulfide layers similar to those in  $\text{Y}_2\text{Ti}_2\text{O}_5\text{S}_2$ , including members of the Ruddlesden–Popper homologous series  $\text{Ba}_{1+x}\text{Zr}_x\text{S}_{3x+1}$  ( $n = 1, 2$ )<sup>23</sup> or the PbFCl-type compound  $\text{ZrSiS}$ ,<sup>24</sup> by these routes have so far proved unsuccessful, possibly because of the resistance of  $\text{Zr}^{4+}$  to reduction in this manner.

**Acknowledgment.** We thank the U.K. EPSRC (Grant GR/N18758) for funding and access to ISIS. We are grateful to Dr. Ron Smith for assistance with measurements carried out at ISIS. S.J.C. thanks the Royal Society for further financial support.

IC0301730

(23) Saeki, M.; Yajima, Y.; Onoda, M. *J. Solid State Chem.* **1991**, *92*, 286.

(24) Onken, H.; Vierheilig, K.; Hahn, H. *Z. Anorg. Allg. Chem.* **1964**, *333*, 266.